Comparison of Sanchez–Lacombe and SAFT Model in Predicting Solubility of Polyethylene in High-Pressure Fluids

YAN XIONG and ERDOGAN KIRAN*

Department of Chemical Engineering, University of Maine, Orono, Maine 04469-5737

SYNOPSIS

Sanchez–Lacombe and SAFT (statistical associating fluid theory) models are used to describe phase behavior of polyethylene solutions (M_w = 2,150, 16,400, 108,000, and 420,000, and M_w/M_n = 1.14, 1.16, 1.32, and 2.66, respectively) in *n*-pentane and in *n*-butane at high pressures. In order to test the predictive capability of the two models, all the predictions were conducted without any adjustment of the binary interaction parameter. Even though both models correctly predict the general trends of the phase envelopes and the LCST (lower critical solution temperature) nature of the systems, SAFT gives predictions that are much closer to the experimental data than the Sanchez–Lacombe model. © 1995 John Wiley & Sons, Inc.

INTRODUCTION

The thermodynamic models for polymer solutions that are being used in practice basically belong to two categories, lattice models and perturbation models. In lattice models, the molecules are assumed to have one or more segments, and the partition function of the system can be obtained by counting the possible configurations when these segments are arranged in hypothetical cells that are like the lattices in the solid materials. Then, the thermodynamic quantities can be calculated from the partition function on the basis of statistical mechanics. A number of models reported in the literature are based on this approach.[1-18] In our previous articles,[19-21] we evaluated the applicability of lattice models for polymer solutions under high pressure and used the Sanchez–Lacombe model as an example to model polyethylene (PE)/*n*-alkane solutions. The calculations show that the Sanchez–Lacombe model can correlate the experimental data for a range of molecular weights if one of the characteristic parameters, i.e. characteristic temperature of PE, is modified by fitting the solubility data for the polymer/*n*-alkane binary mixture at only one molecular weight. However, if the characteristic parameters determined from pressure–volume–temperature (PVT) data for the pure polymer are used directly, the predictions are far from the experimental values.

The perturbation model stems from modern perturbation theory in quantum mechanics, but its basic methodology is simple. First, an idealized system is used as a reference system. This reference system, which should characterize the essential features of the system, is usually obtained by using some theory with well-defined assumptions. The difference between the real system and the ideal system (i.e., reference system) is then accounted for by some correction terms, which are called perturbation terms and are often based on semitheoretical models. The complexity and the magnitude of these perturbation terms depend on the degree of accuracy with which the reference term representing the ideal system can be specified. Based on this methodology, Beret and Prausnitz[22] and Donohue and Prausnitz[23] utilized the results by Carnahan and Starling[24] for hard spheres that can be characterized by square-well potential to describe the reference state and proposed the so-called perturbed hard chain theory (PHCT). Morris et al.[25] modified PHCT by replacing the original perturbation for the square-well potential by a perturbation for the Lennard–Jones potential. This modification is known as perturbed soft chain theory (PSCT). A further refinement, PACT (per-

* To whom correspondence should be addressed.

Journal of Applied Polymer Science, Vol. 55, 1805–1818 (1995)
 CCC 0021-8995/95/131805-14

turbed anisotropic chain theory) was made by Vimalchand et al.[26,27] who incorporated the contributions of anisotropic forces calculated from a perturbation expansion of Gubbins and Twu[28] for anisotropic multipolar interactions and the contributions of isotropic forces calculated as perturbation for the Lennard–Jones potential. Other examples among numerous modifications to PHCT are the simplified perturbed hard chain theory (SPHCT) by Kim et al.[29,30] and the chain of rotators (COR) equation of state by Chien et al.[31]

More recently, a new model that also belongs to the family of perturbation models was developed by Chapman et al.[32–34] and Huang and Radosz.[35,36] This model is known as SAFT or statistical associating fluid theory. The theory is based on the Wertheim's cluster expansion theory[37–39] of which the key result is a relationship between the residual Helmholtz free energy due to association and the monomer density. This monomer density, in turn, is related to a function Δ characterizing the "association strength." Chapman et al. derived the expression for the Helmholtz free energy of this new reference fluid and tested their results against Monte Carlo simulations. Because this new reference fluid incorporates both the chain length (molecular size and shape) and molecular association, the theory is expected to be able to describe most of the real fluids including polymer and polar fluids.[35,36] In the SAFT model, the perturbation term used by Huang and Radosz is the same as the one based on the results proposed by Alder et al.[40] that was used in PHCT by Beret and Prausnitz[22] and in BACK (i.e., Boublik–Alder–Chen–Kreglewski) theory by Chen and Kreglewski.[41]

In this article the predictions by Sanchez–Lacombe and SAFT models are presented for PE/*n*-pentane and PE/*n*-butane systems and the predictive capability of these models is compared.

MODELS

Sanchez–Lacombe Model

Detailed description of the Sanchez–Lacombe model can be found in the literature.[13–18] It is a lattice-fluid model in which vacancies are introduced to account for the compressibility and density changes. The basic equation of state is given by

$$\tilde{\rho}^2 + \tilde{p} + \tilde{T}[\ln(1 - \tilde{\rho}) + (1 - 1/r)\tilde{\rho}] = 0 \quad (1)$$

where $\tilde{p}$, $\tilde{T}$, and $\tilde{\rho}$ are the reduced pressure, temperature, and density respectively, and r represents the number of lattice sites occupied by a molecule. The reduced parameters for a pure substance are defined as $\tilde{p} = p/p^*$, $\tilde{T} = T/T^*$, and $\tilde{\rho} = \rho/\rho^*$ where p^*, T^*, and ρ^* are characteristic pressure, temperature, and density. For mixtures, one additional adjustable parameter, i.e., interaction parameter δ_{ij}, is introduced for each binary pair. This is the only adjustable parameter in the model. The calculation procedure to generate the phase diagrams is described in our previous publications.[19–21]

SAFT

As described in detail by Huang and Radosz,[35,36] the residual Helmholz free energy is the sum of the reference term and dispersion term (perturbation term):

$$a^{\text{res}} = a^{\text{ref}} + a^{\text{disp}} \quad (2)$$

in which the reference term is a sum of the hard-sphere, chain, and association contributions

$$a^{\text{ref}} = a^{\text{hs}} + a^{\text{chain}} + a^{\text{assoc}}. \quad (3)$$

In this model, for a pure substance without association, three characteristic parameters are used for the description, i.e., segment volume v^{00}, segment energy u^0, and segment number m. For self-associating substances, two more parameters ε^{AA} and κ^{AA} are used to account for the association of the molecules. Here, ε^{AA} characterizes the association energy (potential well depth) and κ^{AA} characterizes the association volume (corresponding to the well width r^{AA}). The characteristic parameters for pure substances are determined by optimizing the predictions of vapor–liquid equilibrium (VLE) data. When VLE data is not available, which is the case for polymers, PVT data are used instead. Huang and Radosz[35,36] categorized most of the hydrocarbons into several typical classes and give the general correlation formula of characteristic parameters for each class. For a substance in a given class, these correlation formulas are only functions of the molecular weight. This means that, if there are no accurate PVT data available, the characteristic parameters can be estimated from the molecular weight only. This is a nice feature of SAFT. When SAFT is extended to the mixtures, only one binary mixture parameter is needed. This parameter in SAFT is temperature independent in contrast to most of the lattice theories in which the interaction parameters are temperature dependent.

For mixtures, either volume fraction mixing rules or the van der Waals one-fluid (VDW1) mixing rules

can be used in the model. In our calculations, VDW1 mixing rules are employed and they are given in the following outlines.

The dispersion energy of interaction, u/RT, between segments is given by

$$\frac{u}{RT} = \frac{\sum_i \sum_j X_i X_j m_i m_j \left[\frac{u_{ij}}{RT}\right] v_{ij}^0}{\sum_i \sum_j X_i X_j m_i m_j v_{ij}^0}, \quad (4)$$

where X_i and m_i are the mole fraction and molecular segment number of component i in the mixture. Here, v_{ij}^0 is the segment molar volume for the mixture and is given by

$$v_{ij}^0 = \{\tfrac{1}{2}[(v_i^0)^{1/3} + (v_j^0)^{1/3}]\}^3 \quad (5)$$

in which v_i^0 is temperature dependent segment molar volume and is related to temperature independent segment molar volume v_i^{00} by

$$v^0 = v^{00}[1 - C \exp(-3u^0/RT)]^3, \quad (6)$$

where C is a constant and u^0 is the temperature independent segment energy.

The pair-wise interaction energy term u_{ij} is given by

$$u_{ij} = (u_i u_j)^{1/2}(1 - k_{ij}) \quad (7)$$

in which k_{ij} is an adjustable binary parameter and u_i, the temperature dependent segment energy, in turn is related to u_i^0 by

$$u_i = u_i^0[1 + e/(kT)], \quad (8)$$

where e/k is a constant.

The segment number m for the mixture is expressed as

$$m = \sum_i X_i m_i. \quad (9)$$

In the present system of PE/n-alkane solutions, there are no specific interactions that can lead to molecular association, and therefore the association term in eq. (3) is not considered. The details of the procedure that we have used in this study to calculate the phase boundaries by SAFT are described in the Appendix.

EXPERIMENTAL

The experimental data were obtained by using a variable-volume view cell.[42] The data used in present modeling work has been reported in our previous publications.[19-21,42] Experimental measurements were carried out with four PE standard samples with narrow molecular weight distributions (M_w = 2,150, 16,400, 108,000, and 420,000, with M_w/M_n = 1.14, 1.16, 1.32, 2.66, respectively). The solvents n-pentane (> 99% purity) and n-butane (> 95% purity) were obtained from Aldrich and Matheson, respectively.

The characteristic parameters for the Sanchez–Lacombe model are shown in Table I. Two values of characteristic temperature are given for PE: 650 K is reported based on the PVT data for pure polymer[14] and 521 K specifically obtained by fitting the solubility data of PE/n-pentane binary mixture at 16,400 molecular weight.[19] The characteristic parameters for the SAFT model are given in Table II.

RESULTS AND DISCUSSION

PE/n-Pentane Systems

In the modeling of polymer solutions, or even more generally speaking, in the modeling of any solutions, one of the most challenging problems is to answer the following question. With very little information about the mixture (or without any *a priori* information about the mixture at all) and that only from the thermodynamic data about the pure components, how well can a model predict the phase behavior under wide pressure and temperature conditions? This predictive capability is a very important criterion to judge the performance of a thermodynamic model, because a reliable model with such quality can greatly reduce the experimental effort especially for polymer solutions and blends un-

Table I Characteristic Parameters Used in Sanchez–Lacombe Model

	Parameters		
	P^* (MPa)	T^* (K)	ρ^* (g/cm^3)
n-Pentane[a]	310.1	441	0.755
n-Butane[a]	322.0	403	0.736
Polyethylene	359.0[a]	650[a], 521[b]	0.895[a]

[a] See Sanchez and Lacombe.[14]
[b] See Kiran, Xiong, and Zhuang.[19]

Table II Characteristic Parameters Used in SAFT Model

	Parameters		
Component	m	v^{00} (mL/mol)	u^0/R (K)
n-Alkane[a]	$0.70402 + 0.046647M_w$	$(11.888 + 0.55187M_w)/m$	$210.0 - 26.886 \exp(-0.013341M_w)$
PE[a]	$0.05096M_w$	12.0	210

[a] See Huang and Radosz.[35]

der high pressure and offer a correct guideline for practical applications. In the present study, in order to test the predictive capability of the models, the adjustable parameters (δ_{ij} in the Sanchez–Lacombe model and k_{ij} in SAFT) were fixed at zero and not permitted any further variations.

Figure 1 shows the predictions of $P - X$ curves by the Sanchez–Lacombe model for the PE/n-pentane system at different molecular weights (M_w = 2,150, 16,400, 108,000, and 420,000) at 460 K. The characteristic temperature used in these calculations is 650 K (see Table I) based on the PVT data of PE. Symbols are experimental demixing pressures (i.e., cloud points). Solid and dashed lines represent the Sanchez–Lacombe model predictions for the binodal and spinodal envelopes, respectively. The region above each binodal curve is the one-phase region. As shown from this figure, the general trends of the phase envelopes are correctly predicted by the model: the demixing pressures are increased upon increase of the polymer molecular weight while the critical concentrations shift to lower polymer concentrations. However, the predictions greatly overestimate the experimental values at all molecular weights, with relative average absolute deviations (RAAD[†]) > 200%. Because this large deviation cannot be eliminated by simply adjusting the interaction parameter δ_{ij} alone, a modified value of characteristic temperature 521 K (see Table I) was used in further calculations. This value of 521 K is based on the

[†] RAAD is defined as

$$\text{RAAD} = \sum_i \frac{|S_i^{\text{pred}} - S_i^{\text{exp}}|}{S_i^{\text{exp}}} \times 100\%,$$

where S is the physical quantity under consideration and superscripts pred and exp represent predicted and experimental values, respectively.

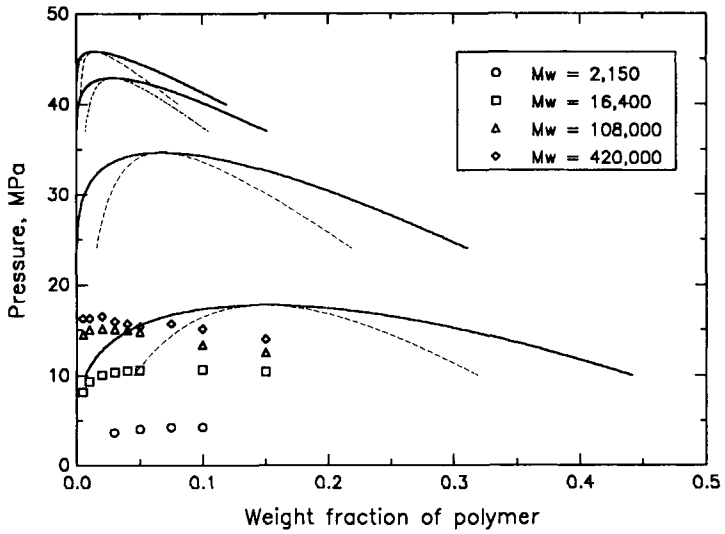

Figure 1 Sanchez–Lacombe model predictions of demixing pressures of PE solutions with polymer concentration and molecular weight at 460 K in n-pentane. Symbols are experimental points; solid lines are calculated binodal envelopes; dashed lines are calculated spinodal envelopes. Characteristic parameters for polymer: P^* = 359 MPa, T^* = 650 K, ρ^* = 0.895 g/cm^3.

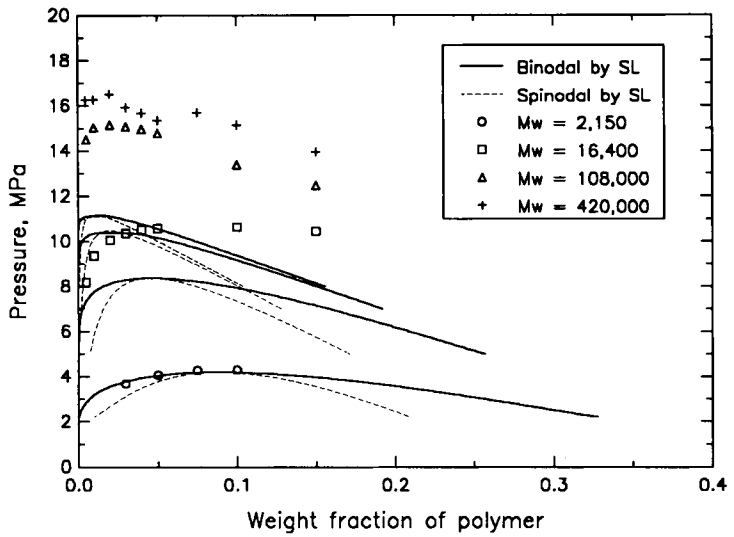

Figure 2 Sanchez–Lacombe model predictions of demixing pressures of PE solutions with polymer concentration and molecular weight at 460 K in *n*-pentane. Symbols are experimental points; solid lines are calculated binodal envelopes; dashed lines are calculated spinodal envelopes. Characteristic parameters for polymer: P^* = 359 MPa, T^* = 521 K, ρ^* = 0.895 g/cm^3.

solubility data for PE of molecular weight 16,400 in *n*-pentane. The optimization procedure is a two-dimensional searching process for both characteristic temperature T^* and interaction parameter δ_{ij} simultaneously in order to obtain a best fit for the solubility data. As described in our previous publications,[19] using this modified value of T^*, the predictions can be greatly improved at all molecular weights by proper adjustments of the interaction parameter δ_{ij}. In the present analysis, even though we use the same value of characteristic temperature 521 K, we do not permit δ_{ij} to vary and set it at δ_{ij} = 0. This would result in deviations on the predictions, even for the 16,400 molecular weight sample, but it permits a complete comparison for the two models.

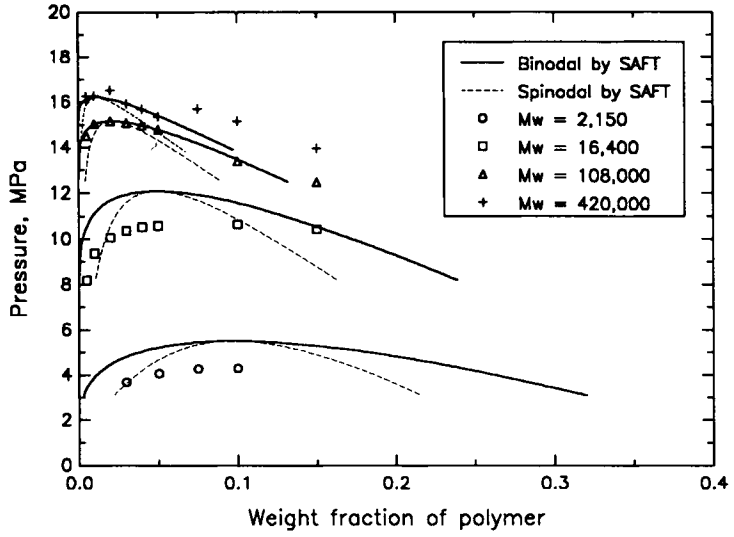

Figure 3 SAFT predictions of demixing pressures of PE solutions with polymer concentration and molecular weight at 460 K in *n*-pentane. Symbols are experimental points; solid lines are calculated binodal envelopes; dashed lines are calculated spinodal envelopes.

Table III Critical Concentrations

		Crit Polymer Conc (wt % Polymer)			
		Molecular Weight			
System	Model	2,150	16,400	108,000	420,000
PE/*n*-pentane	SL	7.3–10.6	4.5–4.7	1.7–2.3	0.7–1.6
	SAFT	8.9–10.6	4.5–5.4	2.0–2.3	1.0–1.3
PE/*n*-butane	SL	10.9–13.0	5.4–5.6	2.3–2.4	1.1–1.3
	SAFT	10.5–11.9	4.9–5.7	2.0–2.5	1.0–1.3

Estimations by Sanchez–Lacombe and SAFT models for the interval in which the critical polymer concentration is located.

With the modified value of characteristic temperature and the value of $\delta_{ij} = 0$, the predictions at 460 K are shown for different molecular weight samples in Figure 2. Although the predictions match the experimental data for the sample with 2,150 molecular weight quite well, the model now underestimates the demixing pressures for high molecular weight samples. The relative deviation for the case of 16,400 molecular weight sample is 2.3 MPa or about 20%, and for the 108,000 and 420,000 molecular weights the deviations are about 5 MPa or 30%. These deviations, even though large, represent great improvement over 200% deviations observed in Figure 1.

Figure 3 is a plot similar to Figures 1 and 2, but shows the predictions by the SAFT model. As shown in this figure, SAFT gives generally good predictions that are very close to the experimental data, especially for high molecular weight samples. The average deviations for 2,150 and 16,400 molecular weight samples are 1.2 and 1.3 MPa, or 30 and 12%, respectively. For the high molecular weight samples, the predictions are remarkably good with deviations of 0.2 MPa or 2% for the 108,000 molecular weight sample, and 0.4 MPa or 3% for the 420,000 molecular weight sample.

It is quite noteworthy to point out that both models predict similar values for the critical concentrations (see Table III). For the same molecular weight samples, remarkable similarities are also observed for the magnitude of the metastable gaps between binodal and spinodal envelopes disregarding the ab-

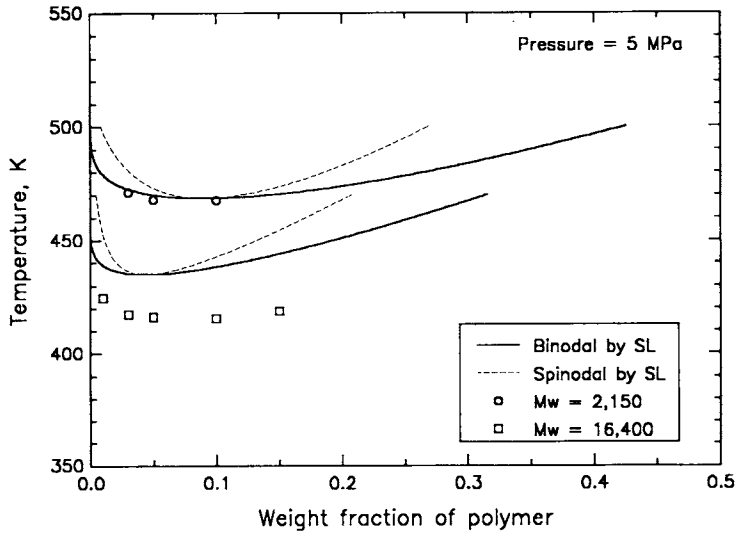

Figure 4 Sanchez–Lacombe model predictions of demixing temperatures of PE solutions with polymer concentration and molecular weight at 5 MPa in *n*-pentane. Symbols are experimental points; solid lines are calculated binodal envelopes; dashed lines are calculated spinodal envelopes. Characteristic parameters for polymer: $P^* = 359$ MPa, $T^* = 521$ K, $\rho^* = 0.895$ g/cm^3.

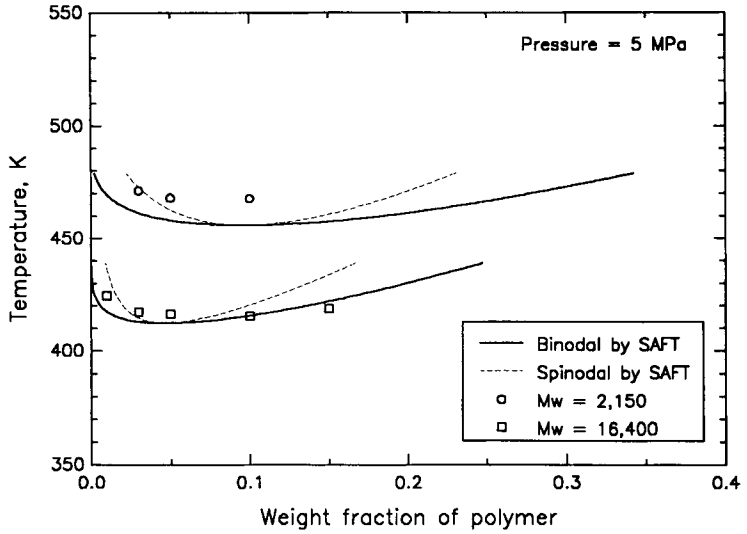

Figure 5 SAFT predictions of demixing temperatures of PE solutions with polymer concentration and molecular weight at 5 MPa *n*-pentane. Symbols are experimental points; solid lines are calculated binodal envelopes; dashed lines are calculated spinodal envelopes.

solute positions of these phase envelopes in the $P - X$ plane. Because of these similarities, either model prediction could be used to evaluate the location of the critical concentrations and also the spinodal from the binodal or vice versa. Using a relatively new technique known as the multiple rapid pressure drop technique (MRPD),[43] information on spinodals should be accessible in the near future for comparisons and assessment of quantitative aspects of the predictions of the gaps between the binodal–spinodal envelopes.

Figures 4 and 5 are predictions of $T - X$ curves at 5 MPa for the two molecular weight samples (M_w = 2,150 and 16,400) by Sanchez–Lacombe and SAFT models, respectively. Both models predict the (lower critical solution temperature (LCST) nature of the system and the decreasing nature of the demixing temperatures with increasing molecular weight. Ac-

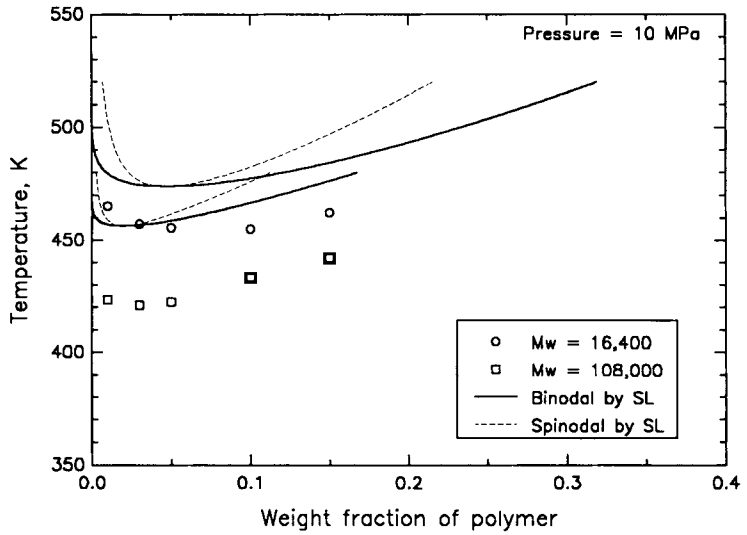

Figure 6 Sanchez–Lacombe model predictions of demixing temperatures of PE solutions with polymer concentration and molecular weight at 10 MPa in *n*-pentane. Symbols are experimental points; solid lines are calculated binodal envelopes; dashed lines are calculated spinodal envelopes. Characteristic parameters for polymer: P^* = 359 MPa, T^* = 521 K, ρ^* = 0.895 g/cm^3.

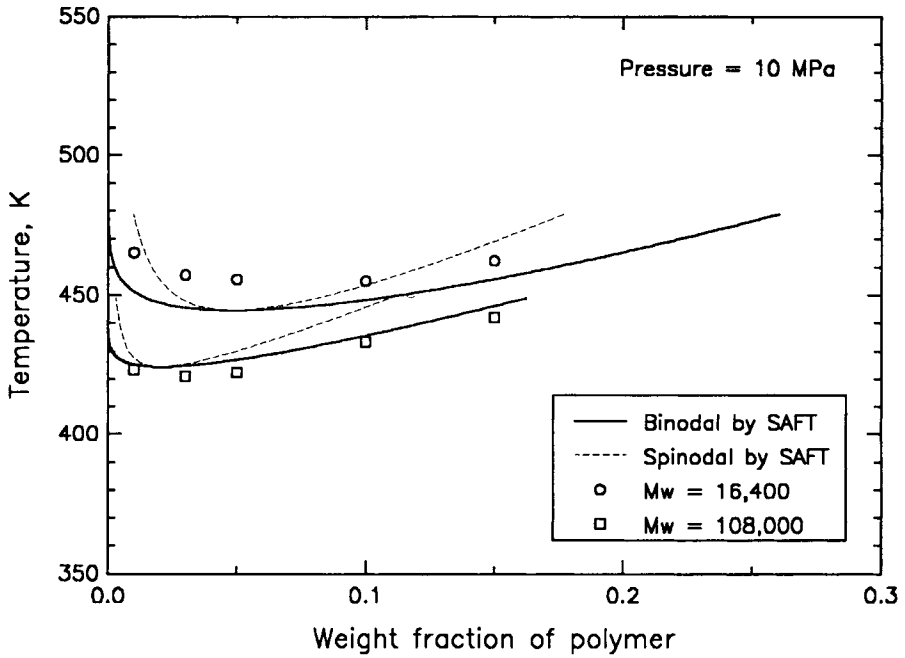

Figure 7 SAFT predictions of demixing temperatures of PE solutions with polymer concentration and molecular weight at 10 MPa *n*-pentane. Symbols are experimental points; solid lines are calculated binodal envelopes; dashed lines are calculated spinodal envelopes.

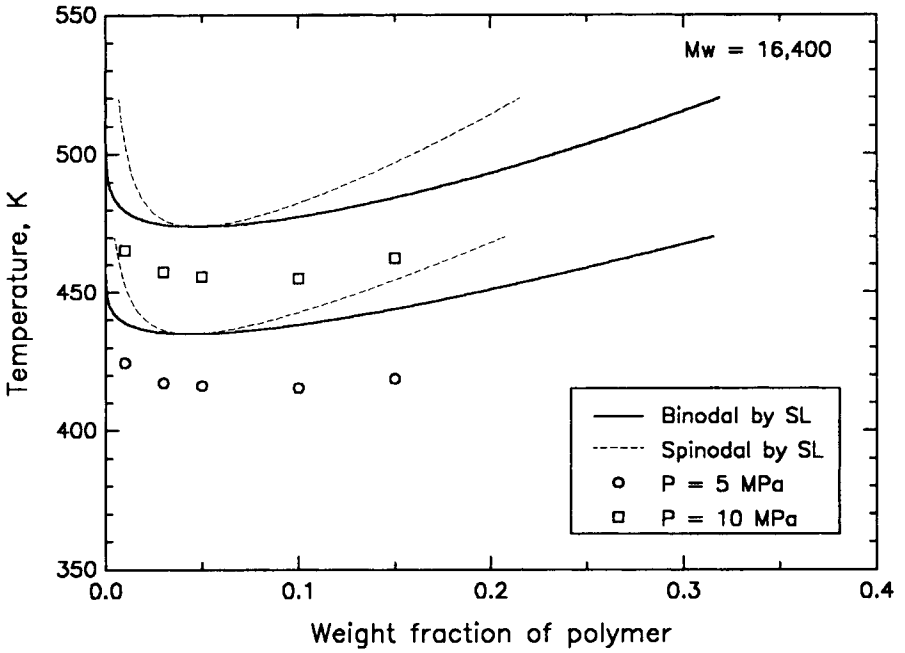

Figure 8 Sanchez–Lacombe model predictions of demixing temperatures of PE solutions with polymer concentration for 16,400 molecular weight sample at different pressures in *n*-pentane. Symbols are experimental points; solid lines are calculated binodal envelopes; dashed lines are calculated spinodal envelopes. Characteristic parameters for polymer: P^* = 359 MPa, T^* = 521 K, ρ^* = 0.895 g/cm^3.

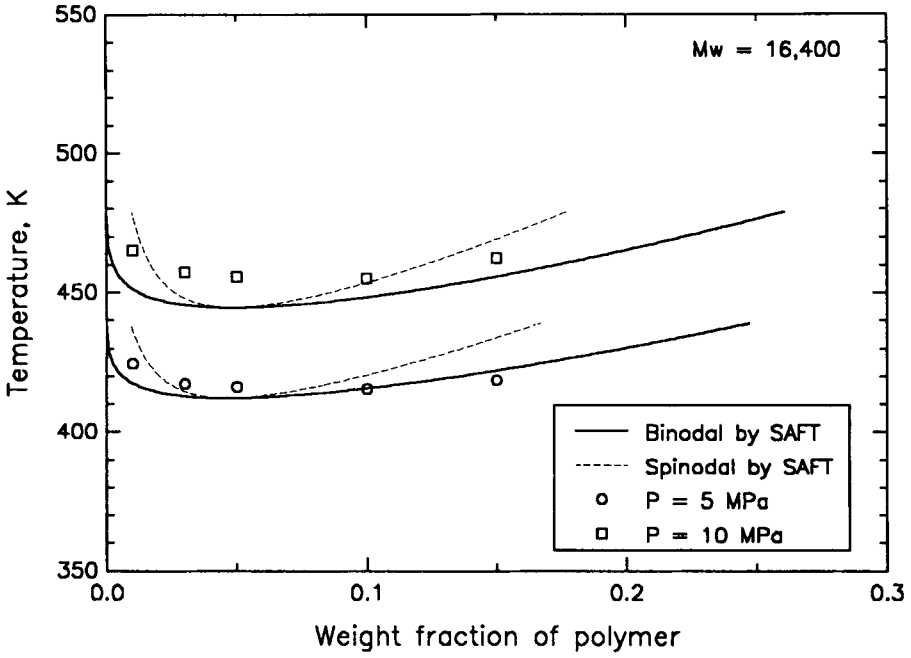

Figure 9 SAFT predictions of demixing temperatures of PE solutions with polymer concentration for 16,400 molecular weight sample at different pressures in *n*-pentane. Symbols are experimental points; solid lines are calculated binodal envelopes; dashed lines are calculated spinodal envelopes.

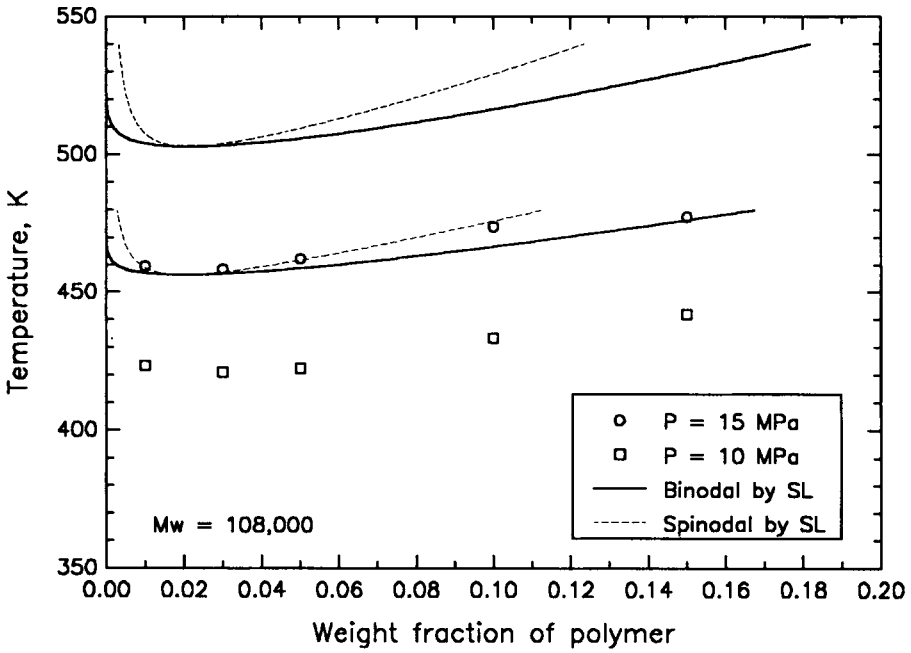

Figure 10 Sanchez–Lacombe model predictions of demixing temperatures of PE solutions with polymer concentration for 108,000 molecular weight sample at different pressures in *n*-pentane. Symbols are experimental points; solid lines are calculated binodal envelopes; dashed lines are calculated spinodal envelopes. Characteristic parameters for polymer: P^* = 359 MPa, T^* = 521 K, ρ^* = 0.895 g/cm^3.

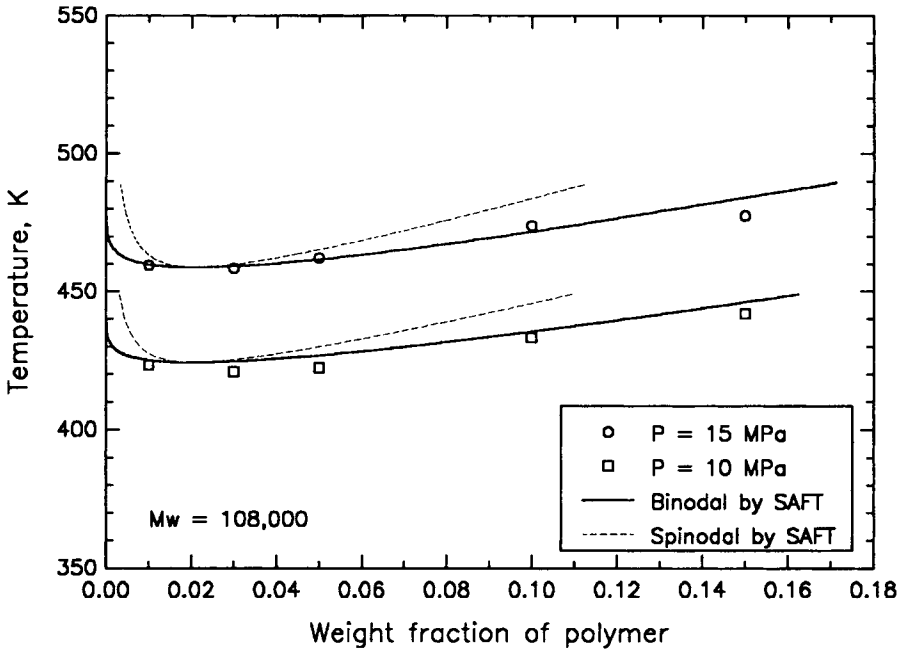

Figure 11 SAFT predictions of demixing temperatures of PE solutions with polymer concentration for 108,000 molecular weight sample at different pressures in *n*-pentane. Symbols are experimental points; solid lines are calculated binodal envelopes; dashed lines are calculated spinodal envelopes.

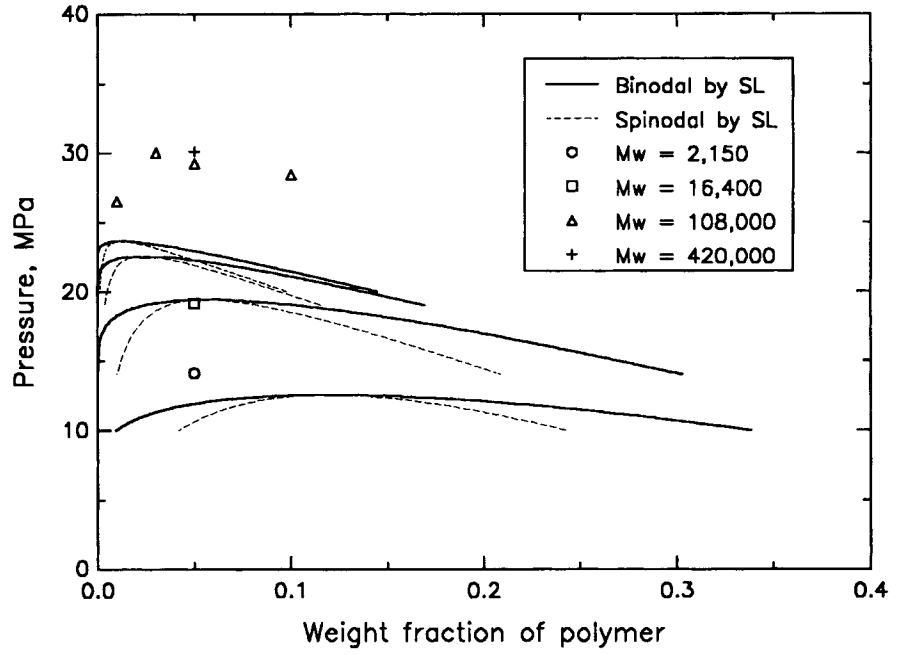

Figure 12 Sanchez–Lacombe model predictions of demixing pressures of PE solutions with polymer concentration and molecular weight at 460 K in *n*-butane. Symbols are experimental points; solid lines are calculated binodal envelopes; dashed lines are calculated spinodal envelopes. Characteristic parameters for polymer: P^* = 359 MPa, T^* = 521 K, ρ^* = 0.895 g/cm^3.

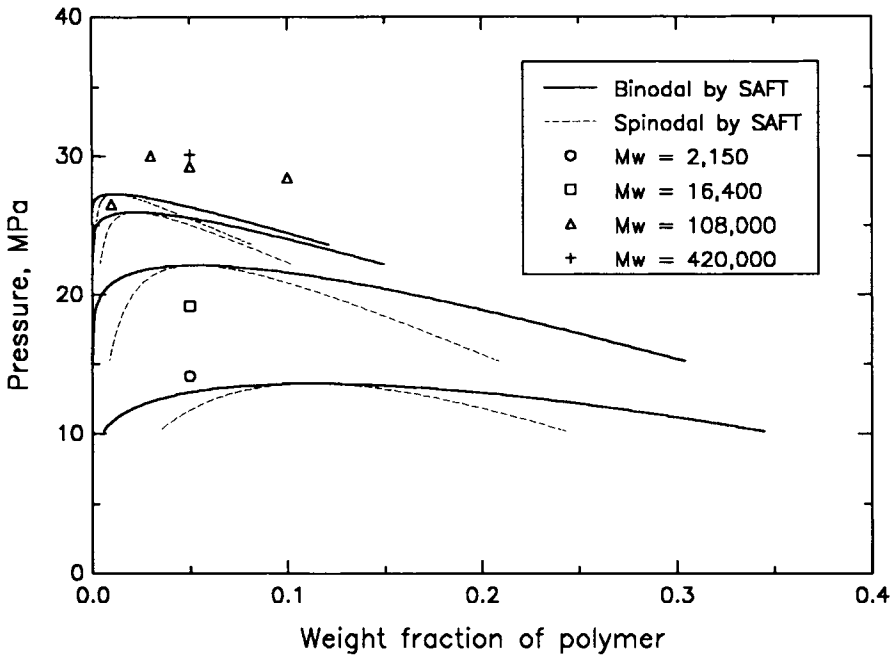

Figure 13 SAFT predictions of demixing pressures of PE solutions with polymer concentration and molecular weight at 460 K in *n*-butane. Symbols are experimental points; solid lines are calculated binodal envelopes; dashed lines are calculated spinodal envelopes.

curacy of the predictions by either model appears comparable under these relatively low pressure conditions, but SAFT appears to be better with high molecular weight and Sanchez–Lacombe model better with low molecular weights. This becomes more apparent at high pressures as shown in Figures 6 and 7. For relatively high molecular weight samples (M_w = 16,400 and 108,000), the predictions by the Sanchez–Lacombe model become poor, whereas the predictions by SAFT are still reasonable. SAFT clearly provides good predictions over a wide range of molecular weights. It is possible that with the Sanchez–Lacombe model, by adapting a different characteristic temperature for the polymer (based on the data for higher molecular weight polymer samples instead of the 16,400 molecular weight sample used in determining the value of 521 K), the predictions may be improved for the higher molecular weight samples. However, this may be at the expense of lowering the predictive power at lower molecular weights. In this respect, the predictive power of the Sanchez–Lacombe model may be limited to a narrowly defined range of molecular weights for quantitatively reliable predictions.

Figures 8–11 show the predictions of $T - X$ curves by the two models for a given molecular weight sample at different pressures. For a 16,400 molecular weight sample, the predictions by the Sanchez–Lacombe model (Fig. 8) are about 20 K or 5% off the experimental data for both pressures 5 and 10 MPa. In contrast, the predictions by SAFT (Fig. 9) are within about 10 K or 2% with experimental data at 10 MPa, and within about 5 K or 1% at 5 MPa. In view of the fact that the characteristic temperature for the Sanchez–Lacombe model was fitted from the data of the 16,400 molecular weight sample in *n*-pentane, and the characteristic parameters for SAFT are obtained only from PVT data for the pure polymer, the poor predictions by the Sanchez–Lacombe model for this molecular weight sample is surprising. The differences in the predictive power of the two models become even greater at higher molecular weights. As shown in Figure 10, the predictions by the Sanchez–Lacombe model are far off from the experimental data (over 40 K difference or 10%), whereas the predictions by SAFT are in remarkable agreement with the experimental data; for both 10 and 15 MPa the deviation of the predictions are less than 5 K or 2%.

In the foregoing analysis, the binary mixture parameter δ_{ij} or k_{ij} were not adjusted in either model. With fine adjustments of δ_{ij}, the predictions by the Sanchez–Lacombe model can be easily improved.[19–21] With similar adjustments on k_{ij}, the predictions by the SAFT model could also be improved. These were not carried out with SAFT because the primary focus

of the present analysis has been to compare the two models without any manipulations.

PE/*n*-Butane System

Figures 12 and 13 show the results of the predictions for the PE/*n*-butane systems. Figure 12 shows the predictions of $P - X$ curves by the Sanchez–Lacombe model for the same polymer samples in this solvent. The accuracy of the predictions is comparable to the case for the PE/*n*-pentane system shown in Figure 2. Predictions by SAFT are shown in Figure 13. Although here the results are not as good as in the case of the PE/*n*-pentane system shown in Figure 3, the overall predictions are consistent and the deviations for all the molecular weights are about 4 MPa or within 20%. As stated above, it should be possible to improve these predictions by allowing the binary mixture parameter to have values other than zero.

As in the case of PE/*n*-pentane solutions, both models give comparable values for the critical polymer concentrations in the PE/*n*-butane systems. The estimations of the critical concentrations for these systems by these models are also given in Table III.

CONCLUSION

It is shown that both Sanchez–Lacombe and SAFT models predict the qualitative aspects of $P - X$ or $T - X$ diagrams for PE/*n*-alkane solutions. They predict similar magnitudes for the miscibility gaps and also for the critical polymer concentrations. However, compared to the predictions by the Sanchez–Lacombe model, the SAFT model predictions are found to be much closer to the experimental data over a wider range of molecular weights.

APPENDIX: CALCULATION OF PHASE BOUNDARIES USING SAFT

After Topliss,[44] Huang and Radosz[35,36] parameterized the expression for the Helmholtz free energy by eight parameters A–H which are defined as:

$$A = \sum_i X_i m_i (d_i)^0 \quad \zeta_0 = (\pi/6)\rho A \tag{A.1}$$

$$B = \sum_i X_i m_i (d_i)^1 \quad \zeta_1 = (\pi/6)\rho B \tag{A.2}$$

$$C = \sum_i X_i m_i (d_i)^2 \quad \zeta_2 = (\pi/6)\rho C \tag{A.3}$$

$$D = \sum_i X_i m_i (d_i)^3 \quad \zeta_3 = (\pi/6)\rho D \tag{A.4}$$

$$E = m = \sum_i \sum_j X_i X_j m_{ij} \tag{A.5}$$

$$F = \frac{a^{\text{chain}}}{RT} = \sum X_i (1 - m_i) \ln(g_{ii}(d_{ii})^{\text{hs}}) \tag{A.6}$$

$$G = \frac{u}{RT} = \frac{\sum_i \sum_j X_i X_j m_i m_j \left[\frac{u_{ij}}{RT}\right] v_{ij}^0}{\sum_i \sum_j X_i X_j m_i m_j v_{ij}^0} \tag{A.7}$$

$$H = \frac{a^{\text{assoc}}}{RT} = \sum_i X_i \left[\sum_{A_i} \left[\ln X^{A_i} - \frac{X^{A_i}}{2} \right] + \frac{1}{2} M_i \right], \tag{A.8}$$

where d is the temperature dependent segment diameter, ρ is the molar density, g is a function of d, X^A is monomer mole fraction (mole fraction of molecules not bonded at site A), M is the molecular weight, and subscripts i or j, represent the ith or jth component in the mixture.

Using the above parameters, the expression for the residual Helmholtz free energy becomes

$$\frac{a^{\text{res}}}{RT} = \frac{\zeta\left[\frac{C^3}{D^2} + \frac{3BC}{D}\right] - \frac{3BC}{D}\zeta^2}{(1-\zeta)^3} - \left[A - \frac{C^3}{D^2}\right]\ln(1-\zeta) + F + E \sum \sum D_{ij} G^i \left(\frac{\zeta}{\tau}\right)^j + H, \tag{A.9}$$

where ζ is equal to ζ_3, and τ and D_{ij} are universal constants. It should be noted that the expression (A.9) above is different from the expression given in the original manuscripts (see equation A24 in Huang and Radosz[35]). Corrections for the original equation appeared in a later publication.[45]

Schematically the residual Helmholtz free energy can be expressed as

$$\frac{a^{\text{res}}}{RT} = f(\rho, A, B, C, D, E, F, G, H), \tag{A.10}$$

where ρ is also included as an independent variable because ζ depends on ρ.

The compressibility factor Z can be expressed as

$$Z = 1 + \rho \left(\frac{\partial\left(\frac{a^{\text{res}}}{RT}\right)}{\partial \rho} \right)_{T,X_i} \tag{A.11}$$

or

$$Z - 1 = \rho\left[\frac{\partial f}{\partial \rho} + \frac{\partial f}{\partial A}\frac{\partial A}{\partial \rho} + \frac{\partial f}{\partial B}\frac{\partial B}{\partial \rho} + \frac{\partial f}{\partial C}\frac{\partial C}{\partial \rho} + \frac{\partial f}{\partial D}\frac{\partial D}{\partial \rho} + \frac{\partial f}{\partial E}\frac{\partial E}{\partial \rho} + \frac{\partial f}{\partial F}\frac{\partial F}{\partial \rho} + \frac{\partial f}{\partial G}\frac{\partial G}{\partial \rho} + \frac{\partial f}{\partial H}\frac{\partial H}{\partial \rho}\right].$$

Because all the partial derivatives of the parameters with respect to ρ go to 0 except for F and H, the above equation can be simplified as

$$Z - 1 = \rho\left[\frac{\partial f}{\partial \rho} + \frac{\partial f}{\partial F}\frac{\partial F}{\partial \rho} + \frac{\partial f}{\partial H}\frac{\partial H}{\partial \rho}\right]. \quad \text{(A.12)}$$

Equation (A.12) essentially is the equation of state expressed by the compressibility for the SAFT model.

The fugacity coefficient used in the calculation of the phase boundaries is given by

$$\ln \varphi_i = \left(\frac{\partial\left(n\frac{a^{res}}{RT}\right)}{\partial X_i}\right)_{\rho,T,X_{j\neq i}} + (Z - 1) - \ln Z, \quad \text{(A.13)}$$

where n is the total number of moles and the first term is given by

$$\left(\frac{\partial\left(n\frac{a^{res}}{RT}\right)}{\partial X_i}\right)_{\rho,T,X_{j\neq i}} = \frac{a^{res}}{RT} + \left(\frac{d\left(\frac{a^{res}}{RT}\right)}{dX_i}\right)_{\rho,T,X_{j\neq i}} - \sum_j X_j\left(\frac{d\left(\frac{a^{res}}{RT}\right)}{dX_j}\right)_{\rho,T,X_{j\neq i}}. \quad \text{(A.14)}$$

From the fugacity coefficient, the equilibrium compositions can be calculated by imposing

$$\varphi_i' X_i' = \varphi_i'' X_i'' \quad \text{(A.15)}$$

where $'$ and $''$ denote different phases and $i = 1, 2, \ldots, l$, and l is the number of the components in the system. The spinodal values were obtained by searching the extreme points of fugacity $f_i = \varphi_i X_i P$. In the actual calculations, an equivalent function $f_i' = \ln \varphi_i + \ln X_i$ was used to facilitate numerical calculations.

The equilibrium compositions were searched simultaneously at fixed temperature and pressure. The solutions of a system of nonlinear equations are solved by a modification of the Powell hybrid method.

REFERENCES

1. P. J. Flory, *J. Chem. Phys.*, **9,** 660 (1941).
2. P. J. Flory, *J. Chem. Phys.*, **10,** 51 (1942).
3. M. L. Huggins, *J. Chem. Phys.*, **9,** 440 (1941).
4. P. J. Flory, *Principles of Polymer Chemistry,* Cornell University Press: Ithaca, New York, 1953.
5. P. J. Flory, R. A. Orwoll, and A. Vrij, *J. Am. Chem. Soc.*, **86,** 3507 (1964).
6. P. J. Flory, R. A. Orwoll, A. Vrij, *J. Am. Chem. Soc.*, **86,** 3515 (1964).
7. R. Simha and T. Somcynsky, *Macromolecules,* **2,** 341 (1969).
8. T. Somcynsky and R. Simha, *J. Appl. Phys.*, **42,** 4545 (1971).
9. G. T. Dee and D. J. Walsh, *Macromolecules,* **21,** 811 (1988).
10. G. T. Dee and D. J. Walsh, *Macromolecules,* **21,** 815 (1988).
11. A. L. Kleintjens and R. Koningsveld, *Colloid Polym. Sci.*, **258,** 711 (1980).
12. A. L. Kleintjens, *Fluid Phase Equilib.*, **10,** 183 (1983).
13. I. C. Sanchez, *Polymer Blends,* D. R. Paul and S. Newman, Eds., Academic Press, New York, 1978, Chap. 3, pp. 115–139.
14. I. C. Sanchez and R. H. Lacombe, *J. Phys. Chem.*, **80**(21), 2352 (1976).
15. R. H. Lacombe and I. C. Sanchez, *J. Phys. Chem.*, **80**(23), 2568 (1976).
16. I. C. Sanchez and R. H. Lacombe, *Macromolecules,* **11**(6), 1145 (1978).
17. I. C. Sanchez, *Encyclo. Phys. Sci. Technol.*, **11,** (1987).
18. C. Panayiotou and I. C. Sanchez, *Macromolecules,* **24,** 6231 (1991).
19. E. Kiran, Y. Xiong, and W. Zhuang, *J. Supercritical Fluids,* **6,** 193 (1993).
20. Y. Xiong and E. Kiran, *Polymer,* **35,** 4408 (1994).
21. Y. Xiong and E. Kiran, *J. Appl. Polym. Sci.*, **53,** 1179 (1994).
22. S. Beret and J. M. Prausnitz, *AIChE J.*, **21,** 1123 (1975).
23. M. D. Donohue and J. M. Prausnitz, *AIChE J.*, **24**(5), 849 (1978).
24. N. F. Carnahan and K. E. Starling, *J. Chem. Phys.*, **51,** 635 (1969).
25. W. O. Morris, P. Vimalchand, and M. D. Donohue, *Fluid Phase Equilib.*, **32,** 103 (1987).
26. P. Vimalchand and M. D. Donohue, *Ind. Eng. Chem. Fundamentals,* **24,** 246 (1985).
27. P. Vimalchand, I. Celmins, and M. D. Donohue, *AICHE J.*, **32,** 1735 (1986).
28. K. E. Gubbins and C. H. Twu, *Chem. Eng. Sci.*, **33,** 3863 (1978).
29. C. H. Kim, P. Vimalhand, M. D. Donohue, and S. I. Sandler, *AICHE J.*, **32,** 1726 (1986).

30. C. H. Kim, W. C. Wang, H. M. Lin, and K. C. Chao, *Ind. Eng. Chem. Fundamentals,* **25,** 75 (1986).
31. C. H. Chien, R. A. Greencorn, and K. C. Chao, *AICHE J.,* **29,** 569 (1983).
32. W. G. Chapman, K. E. Gubbins, G. Jackson, and M. Radosz, *Fluid Phase Equilib.,* **52,** 31 (1989).
33. W. G. Chapman, K. E. Gubbins, C. G. Joslin, and C. G. Gray, *Fluid Phase Equilib.,* **29,** 337 (1989).
34. W. G. Chapman, K. E. Gubbins, G. Jackson, and M. Radosz, *Ind. Eng. Chem. Res.,* **29,** 1709 (1990).
35. S. H. Huang and M. Radosz, *Ind. Eng. Chem.,* **30,** 1994 (1991).
36. S. H. Huang and M. Radosz, *Ind. Eng. Chem.,* **29,** 2284 (1991).
37. M. S. Wertheim, *J. Stat. Phys.,* **35,** 35 (1984).
38. M. S. Wertheim, *J. Stat. Phys.,* **42,** 459 (1986).
39. M. S. Wertheim, *J. Stat. Phys.,* **42,** 477 (1986).
40. B. J. Alder, D. A. Young, and M. A. Mark, *J. Chem. Phys.,* **56,** 3013 (1972).
41. S. S. Chen and A. Kreglewski, *Beriche der Bunsen-Ges. Phys. Chem.,* **81,** 1048 (1970).
42. E. Kiran and W. Zhuang, *Polymer,* **33,** 5259 (1992).
43. E. Kiran and W. Zhuang, *J. Supercritical Fluids,* **7,** 7 (1994).
44. R. J. Topliss, Ph.D. dissertation, University of California, Berkeley, 1985.
45. S. H. Huang and M. Radosz, *Ind. Eng. Chem.,* **32,** 762 (1993).

Received March 28, 1994
Accepted March 28, 1994